processes

MDPI

Article

Artificial Neural Networks for Mineral Production Forecasting in the In Situ Leaching Process: Uranium Case Study

Daniar Aizhulov [1,2,*], Madina Tungatarova [1,3,*], Maksat Kurmanseiit [3] and Nurlan Shayakhmetov [3]

[1] Joldasbekov Institute of Mechanics and Engineering, Almaty 050010, Kazakhstan
[2] Department of Software Engineering, Satbayev University, Almaty 050013, Kazakhstan
[3] Department of Mechanical Engineering, Satbayev University, Almaty 050013, Kazakhstan; m.kurmanseiit@satbayev.university (M.K.); shayakhmetovn@gmail.com (N.S.)
* Correspondence: daniar.aizhulov@gmail.com (D.A.); m.tungatarova@satbayev.university (M.T.)

Abstract: This study was conducted to assess the applicability of artificial neural networks (ANN) for forecasting the dynamics of uranium extraction over exploitation time during the process of In Situ Leaching (ISL). Currently, ISL process simulation involves multiple steps, starting with geostatistical interpolation, followed by computational fluid dynamics (CFD) and reactive transport simulation. While extensive research exists detailing each of these steps, machine learning techniques may offer the potential to directly obtain extraction curves (i.e., the concentration of the mineral produced over the exploitation time of the deposit), thereby bypassing these computationally expensive steps. As a basis, both an empirical experimental configuration and reactive transport simulations were used to generate training data for the neural network model. An ANN was constructed, trained, and tested on several test cases with different initial parameters, then the expected outcomes were compared to those derived from conventional modeling techniques. The results indicate that for the employed experimental configuration and a limited number of features, artificial intelligence technologies, specifically regression-based neural networks can model the recovery rate (or extraction degree) of the ISL process for mineral production, achieving a high degree of accuracy compared to traditional CFD and mass transport models.

Keywords: in situ leaching; mineral extraction; neural networks; production forecasting; machine learning; artificial intelligence

check for updates

Citation: Aizhulov, D.; Tungatarova, M.; Kurmanseiit, M.; Shayakhmetov, N. Artificial Neural Networks for Mineral Production Forecasting in the In Situ Leaching Process: Uranium Case Study. *Processes* **2024**, *12*, 2285. https://doi.org/10.3390/pr12102285

Academic Editor: Jie Zhang

Received: 12 September 2024
Revised: 15 October 2024
Accepted: 17 October 2024
Published: 18 October 2024

Copyright: © 2024 by the authors. Licensee MDPI, Basel, Switzerland. This article is an open access article distributed under the terms and conditions of the Creative Commons Attribution (CC BY) license (https://creativecommons.org/licenses/by/4.0/).

1. Introduction

The application of In Situ Leaching (ISL) techniques has significantly enhanced uranium production in various countries, with Kazakhstan being a prominent example. This method's efficiency and relative safety have contributed to its widespread adoption, leading to increased uranium output on a global scale [1]. The process involves the injection of a leaching solution, typically sulfuric acid, into the subsurface through injection wells. This solution dissolves the crystallized minerals present in the ore body. The resulting pregnant solution is then extracted and brought back to the surface through production wells for further processing [2,3]. However, after the solution is introduced into the subsurface, the hydrodynamic and chemical processes that occur remain hidden. Consequently, forecasting the recovery rate, monitoring solution flows outside the designated block to mitigate environmental impact, and addressing other associated challenges all become significantly more difficult.

Various reactive transport models have been proposed to simulate the ISL process; these involve geostatistical modeling, CFD, and modeling of the kinetics of chemical processes. Verification of such models is a challenge in itself, as empirical data on production regimes (debits, acidity of the solution, location of wells, height and depth of well screens, etc.) and resulting recovery data (recovery rate, well productivity, remaining

leaching solution, etc.) are only available at the surface. For instance, a reactive transport model for simulating the ISL of uranium was proposed in the work of [4]. The model was based on empirical data from laboratory experimentation conducted within JSC NAC Kazatomporm [5,6], which was subsequently verified using data from the Budonovskoye deposit. The hydrodynamics of the ISL process were studied in [7], where the problem of selecting an optimal pumping–injection ratio to prevent groundwater interference between the two well sites was investigated. The work of [8] presented a numerical model of water and solute behavior in a mining area. This study applied three-dimensional reactive transport modeling to develop a pollution control mining plan for ISL of uranium. Additionally, a software complex was developed to simulate ISL process, with geomodeling, CFD, reactive transport, and economic modules [9].

Modeling of the ISL process typically involves the steps laid out below (see Figure 1).

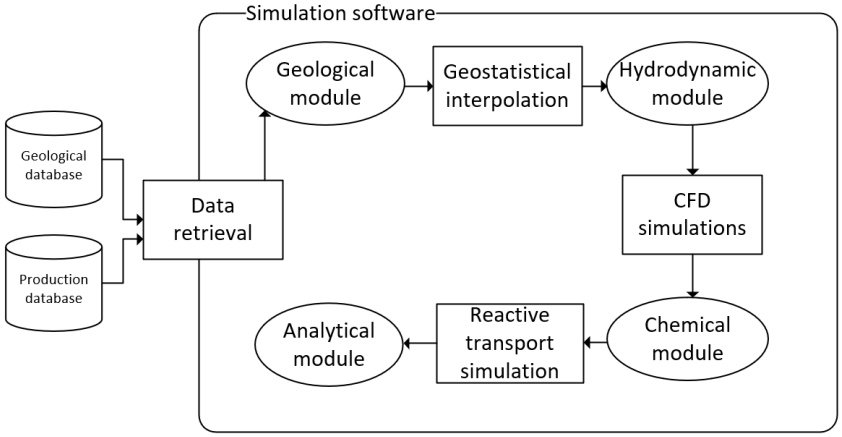


Figure 1. The ISL modeling process involves geological, hydrodynamic, and reactive transport simulations.

1. Retrieving data from geological and production databases for a block under consideration: Geological datasets might include well locations (exploratory, technological, or observational wells), inclinometry, well screen positions and height along the wells, the results of geophysical interpretations in the form of 1D interval data (lithology, filtration properties, mineralization, red-ox conditions, etc). Production datasets might include data regarding changes in technological regimes over time (injection and production debits, concentration of reagent in the leaching solution, presence of intensification compounds, etc.) as well as resulting production data (concentration of the useful component that is being extracted, remaining reagent concentration in the pregnant solution).
2. Well data are interpolated on a custom grid covering the technological block under consideration. Important values include the spatial distribution of mineralization (contributing to reserve estimation) and hydraulic conductivity in each node in the inter-well space. Various studies have been conducted in this field, including geological modeling based on reactive transport simulation of deposit genesis [10], and geostatistical interpolations of well data [11–13].
3. Given the known filtration properties of the domain and the well flow rates, Computational Fluid Dynamics (CFD) methods are employed to determine the pressure and velocity fields. These fields can then be utilized for streamline simulations [14], which in turn provide critical insights into the presence of stagnant mineral volumes or potential spread of the leaching solution beyond the intended technological block boundaries.
4. After the velocity field and the chemical composition of the ore-bearing layer and leaching solution have been established, the kinetics of chemical reactions are modeled to simulate the reactive transport processes [4]. At this stage, the stream lines and

fronts of both leaching and pregnant solutions can be visualized to obtain an overall understanding of the production process. This analysis allows for the identification of potential issues that could decrease the leaching efficiency, such as solution displacement due to gravitational effects [15], gypsum formation [16], or mechanical clogging of pores. Therefore, reactive transport simulation for ISL of uranium must account for the dynamics of injection and pumping, the spatial relationship between the leaching and acidification zones, the volume fraction and reaction rates of uranium ore, potential pore blockage by precipitation, the influence of reinjection fluid components, and the kinetic and thermodynamic aspects of the dissolution processes [17].

5. Extraction curves are constructed for the uranium concentration in a block over time, and the data are analyzed to determine the efficiency of production from an economic standpoint.

The main issue with these simulations is calculation time. As we observed at the mining sites, on a high-end PC it can take up to 20 h to simulate the ISL of a single technological block for an exploitation time of 3–4 years. For a domain with $200 \times 200 \times 200$ nodes, geostatistical interpolation with Kriging algorithm requires up to 10 min, solving elliptic equation with the over-relaxation iterative method requires 5–12 h, and reactive transport simulation can take around 7–8 h [9]. Use of centralized clusters might not be an option due to the data security policies of each mining entity (especially in the case of uranium production) and remoteness of the deposits. Attempts to accelerate the simulation process have been presented in the work of [15], where acceleration by a factor of 33 was realized by GPU computations with CUDA and through parallelization by splitting a 3D problem into a set of 1D problems.

Evidently, the measured computational duration might be acceptable time period for calculations related to retrospective analysis or for efficiently solving particular problems with the technological block. However, with exploratory data at hand, forecasting of various development scenarios before commissioning a new block becomes a challenge.

Artificial neural networks and machine learning techniques have been used to model many complex physical processes in recent years. These methods rely on approximating functions and discovering patterns within large datasets. ANNs require paired input data and expected outcome data for training and testing to assess the effectiveness of the learning process. These data can be obtained from experiments or generated through comprehensive direct simulations, with the latter approach being especially common when utilizing neural networks grounded in the principles of Physics-Informed Neural Networks (PINNs) [18–21].

An idea presented in the current work is to study the applicability of neural network-based models for generating extraction curves and assess the computational speed compared to traditional modeling approaches. Neural networks have been extensively used to simulate production processes [22,23], while Physics-Informed Neural Networks have shown to be a viable approach for imitating physical processes [24,25]. By taking geological and production data as input parameters and feeding the results of traditional modeling into the network as a training data, it might be possible to directly obtain extraction curves, allowing costly intermediate steps to be bypassed.

The reactive transport model proposed in [4] was based on industrial laboratory experiments [5]. This model has been confirmed to provide acceptably accurate results when applied to technological blocks of real uranium deposits in Kazakhstan. In the present work, this model was used to generate training data for an artificial neural network with various input parameters. Separate datasets with different input data (not included in training dataset) were prepared to test the accuracy and error rate of the pretrained neural network.

Synthetic training data were generated using ISL simulation software developed by the authors in C# programming language. The neural network model was developed in Python employing the Keras open-source library (version 2.13.1).

2. Reactive Transport Simulation to Prepare Training Data for Artificial Neural Network

An artificial neural network model was trained to imitate a 1D experiment conducted within JSC NAC Kazatomprom and published in [5]. The training data were generated using the reactive transport model proposed by [4]. In the experiment, a tube with length of 1 m and a diameter of 30 cm is filled with uranium mineral containing fine-grained sandstone of 0.22 porosity. A solution containing sulfuric acid (reagent) is injected into the tube from a Mariotte's vessel, maintaining a constant flow rate. At the end of the tube, the dissolved uranium in the pregnant solution is measured (Figure 2).

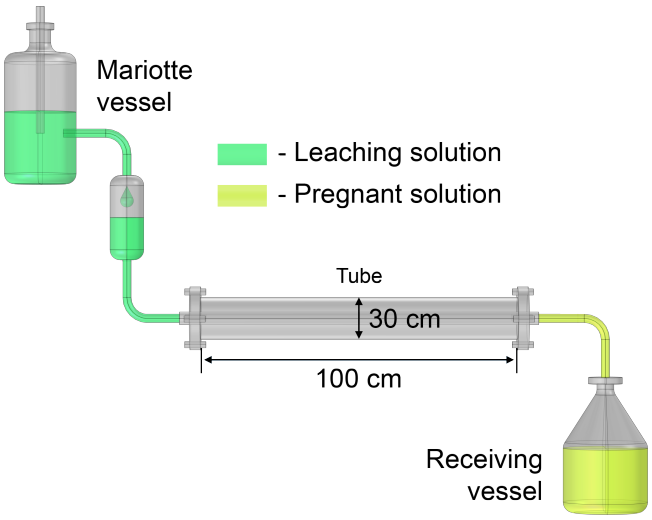


Figure 2. The tube experiment considered in the reactive transport modeling used to generate training data for the ANN.

Given the lack of detailed studies on the composition of the ore-bearing rock, an assumption of the experiment is that uranium in the form of tetravalent $UO_{2(s)}$ and hexavalent uranium $UO_{3(s)}$ compounds is present in equal proportions. During the leaching process, the reagent is consumed through its interaction with the rock. The chemical interaction between the reagent and the rock is described by the following simplified equations :

$$UO_{3(s)} + H_2SO_{4(l)} = UO_2SO_{4(l)} + H_2O_{(l)} \tag{1}$$

$$UO_{2(s)} + H_2SO_{4(l)} = UO_2SO_{4(l)} + 2H^+_{(l)} \tag{2}$$

$$Minerals_s + H_2SO_{4(l)} = Solution_{(l)}. \tag{3}$$

The mathematical model of reactive transport for the system of equations in Equations (1)–(3) is expressed as follows:

$$\partial_t((1-\phi)c_{UO_3}) = -\omega_1 \tag{4}$$

$$\partial_t((1-\phi)c_{UO_2}) = -\omega_2 \tag{5}$$

$$\partial_t((1-\phi)c_{Minerals}) = -\omega_3 \tag{6}$$

$$\partial_t(\phi c_{H_2SO_4}) + \nabla(\phi c_{H_2SO_4}\, v) = \nabla \cdot (\phi D \nabla c_{H_2SO_4}) - [\omega_1 + \omega_2 + \omega_3] \tag{7}$$

$$\partial_t(\phi c_{UO_2SO_4}) + \nabla(\phi c_{H_2SO_4}\, v) = \nabla \cdot (\phi D \nabla c_{H_2SO_4}) + [\omega_1 + \omega_2]. \tag{8}$$

where c denotes the molar concentration [mol·L^{-1}], ϕ is the rock porosity [m^3·m^{-3}], t describes the time [days], ∂_t is the derivative by time [day^{-1}], D is the dispersion coefficient [m^2·day^{-1}], v is is the fluid flow velocity [m·day^{-1}], and ω_i the rate of change of the ith component [mol·L^{-1}·day^{-1}] according to the Law of Mass Action [26,27]:

$$\omega_1 = -k_{U^{VI}} c_{UO_3} c_{H_2SO_4} \omega_2 = -k_{U^{IV}} c_{UO_2} c_{H_2SO_4} \omega_3 = -k_{Minerals} c_{Minerals} c_{H_2SO_4}. \quad (9)$$

The leaching of uranium from a tube is considered with the geometric dimensions and properties of the rock detailed in Table 1. An experimental investigation of uranium leaching from a tube was previously documented by Poezhaev in [5]. In their experiment, a leaching solution with a constant sulfuric acid concentration is continuously introduced at a steady rate into a tube filled with ore rock. The uranium concentration in the solution is measured at the tube's outlet, and extraction curves are subsequently constructed based on these measurements (Figure 2).

Table 1. Constant parameters within the modeling framework used for generating training and testing data.

r [m]	l [m]	ρ_s [kg·m^{-3}]	ρ_l [kg·m^{-3}]	ϕ [m^3·m^{-3}]
0.15	1.0	1700	1015	0.29

r—tube radius, l—tube length.

All simulations used to generate training and testing data were conducted in molar concentrations [mol·L^{-1}], with concentrations for solids determined as $c_u = \rho_s y_u / M_u$, where c_u is molar concentration of uranium, ρ_s is density of solid [kg·m^{-3}], y is the uranium grade [kg·kg^{-1}], and M_u is the molar mass of uranium [g·mol^{-1}]; in addition, $c_{H_2SO_4} = \rho_l y_{H_2SO_4} / M_{H_2SO_4}$ is the formula for determining the molar concentration of reagent, where $\rho_l y_{H_2SO_4}$ is the concentration of reagent (as shown in Table 2).

Table 2. Ranges of variation of input parameters for the model training and testing datasets.

Definition	Designation	Unit	Values		
			From	To	Step
velocity	v	m·day^{-1}	0.5	0.9	0.1
concentration of reagent	$\rho_{H_2SO_{4(l)}} = \rho_l y_{H_2SO_4}$	g·L^{-1}	10	30	5
uranium grade	y_U^0	kg·kg^{-1}	0.00035	0.00055	0.00005

The reaction rate constants (Table 3) shown below were determined in [4].

Table 3. Reaction rate constants.

$k_{U^{(VI)}}$	$k_{U^{(IV)}}$	$k_{U^{Minerals}}$
4.4	0.6	0.5

3. Application of Artificial Neural Networks to Obtain Extraction Curves of Uranium Production with In Situ Leaching Process

3.1. Training the Artificial Neural Network

Conceptually, we presume that the Artificial Neural Network (ANN) should be able to provide the concentration of uranium in pregnant solution in a technological block for a given exploitation time with the provided parameters. In the current work, the aforementioned tube experiment was employed to train an ANN using the following customized input parameters:

- Velocity [m·day^{-1}]
- Reagent concentration [g·L^{-1}]

- Concentration of uranium in the tube [%]
- Time [days]

An output parameter should be the eventual concentration of dissolved uranium in the pregnant solution.

The ANN architecture was designed as follows (Figure 3):

- Four layers, consisting of an input layer, an output layer, and two hidden layers;
- Four nodes per each parameter in the input layer;
- Two hidden layers to account for nonlinearity of the solution, with 64 nodes in each;
- One node (concentration of uranium) in the output layer.

The problem under consideration is inherently nonlinear, necessitating the use of two hidden layers in the neural network to effectively capture the nonlinearity. The selection of the number of neurons in these layers was guided by the relatively low number of features and the size of the available dataset. Expanding the dataset and incorporating additional parameters could require increasing the number of neurons to accurately capture complex patterns; however, this adjustment would likely lead to a tradeoff, as a larger neural network would have increased computational time and resource demands. A sequential neural network model was employed utilizing the rectified linear unit (ReLU) as the activation function. The training process was optimized using the Adam optimization algorithm.

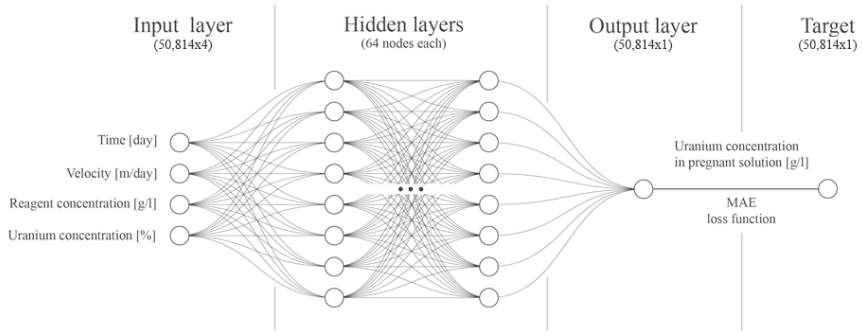


Figure 3. Artificial Neural Network model architecture.

As shown in Table 2, a total of 125 cases was simulated (Figure 4), each covering a time period of 20 days. Of these, three cases were designated as test cases, while the remaining 122 cases were used for model training. Upon merging the training data, the resulting dataset comprised 50,814 rows and four columns. It is important to note that the number of time steps varied across cases due to the adjustments in the time increment (Δt) based on the stability condition.

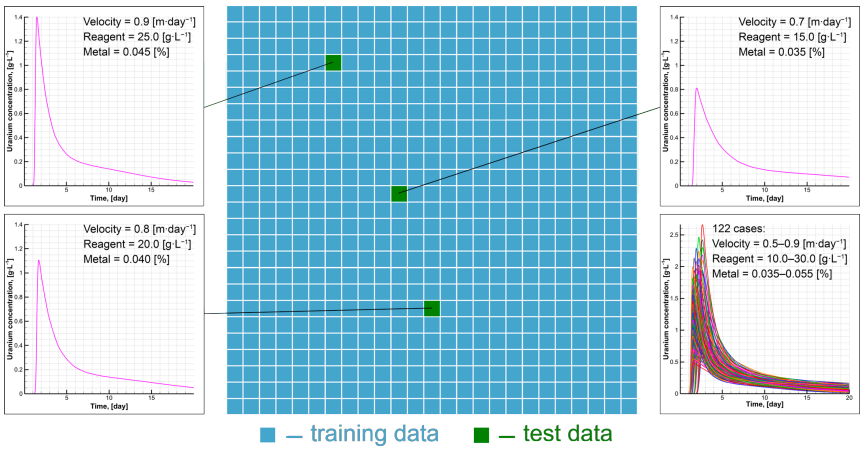


Figure 4. Training data were obtained through reactive transport modeling, with some of the cases being used for testing purposes.

Training the model on this dataset took around 20 min with learning rate of 0.01 and number of epochs equal to 780, resulting in the loss function with MAE shown in Figure 5.

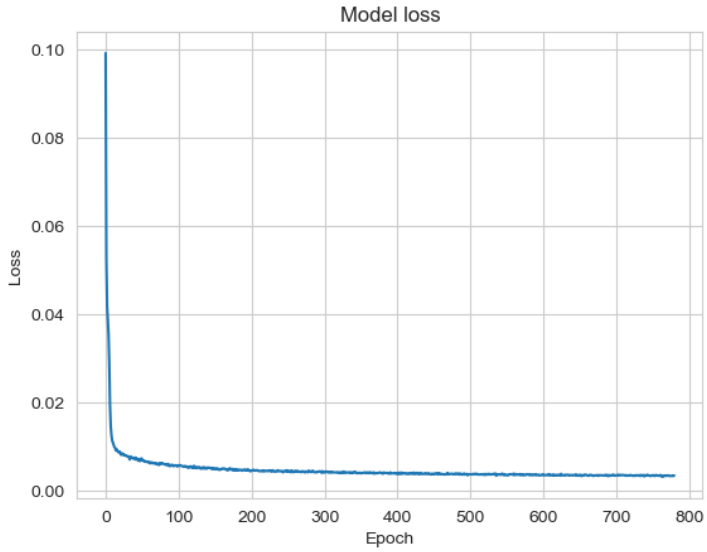


Figure 5. Loss function obtained after training the neural model over 780 epochs.

3.2. Results of Applying the Artificial Neural Network to In Situ Leaching

The model was evaluated on a set of test cases that were not included in the training dataset (Table 4). The following scenarios were considered, along with their corresponding extraction curves: (1) a velocity of 0.7 m per day, sulfuric acid concentration in the leaching solution of 15 g per liter, and solid uranium concentration of 0.035%; (2) a velocity of 0.8 m per day, sulfuric acid concentration in the leaching solution of 20 g per liter, and solid uranium concentration of 0.04%; (3) a velocity of 0.9 m per day, sulfuric acid concentration in the leaching solution of 25 g per liter, and solid uranium concentration of 0.045%.

Table 4. Test cases used to evaluate the prediction accuracy of the ANN.

Case	Velocity v [m·day^{-1}]	Concentration of Reagent [g·L^{-1}]	Solid U Concentration [%]
Case 1	0.7	15	0.035
Case 2	0.8	20	0.04
Case 3	0.9	25	0.045

Figure 6 shows the prediction of the extraction curve (mg·L^{-1} of uranium per day in the pregnant solution in the tube) for test case scenario number 1.

The predictions of the neural network model showed strong alignment with the uranium production data obtained from the numerical tube experiments. The prediction errors for uranium concentration ranged from 0.02257 to 0.02551 mg·L^{-1}. The average absolute error was 0.00037 mg·L^{-1}, for a deviation of 0.02596%. A higher degree of underestimation was observed when the extraction rate began to increase, corresponding to the moment when the pregnant solution reaches the end of the tube, which is analogous to its arrival at the production well. However, as is evident from the chart, this error primarily indicates a shift in the time of the curve towards an earlier time frame. Therefore, a better comparison would be to contrast the integrals of the expected and predicted curves:

$$S_d = \frac{|\int Pdt - \int Edt|}{\int Edt}. \quad (10)$$

where the percentage difference of total produced uranium S_d is equal to the absolute difference between the predicted production P and expected production E. In this case, the difference was equal to 0.17981%.

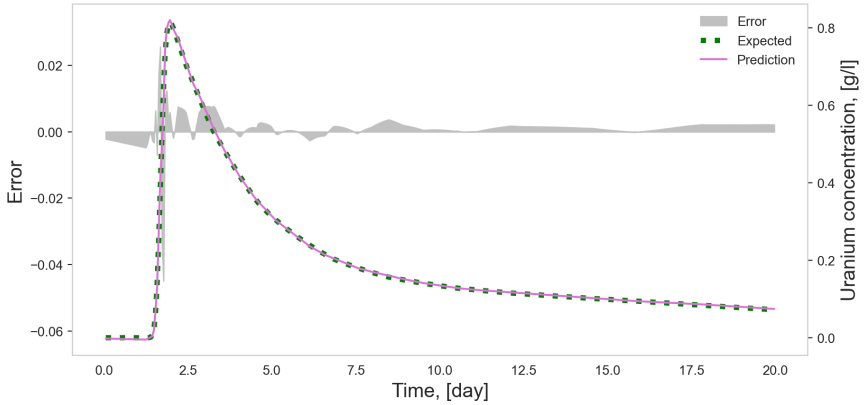


Figure 6. Extraction of uranium prediction for test case 1, with both vertical axes having different scales.

Figure 7 presents the predicted extraction curve, representing the concentration of uranium in the pregnant solution [mg·L^{-1}] per day for test case scenario 2.

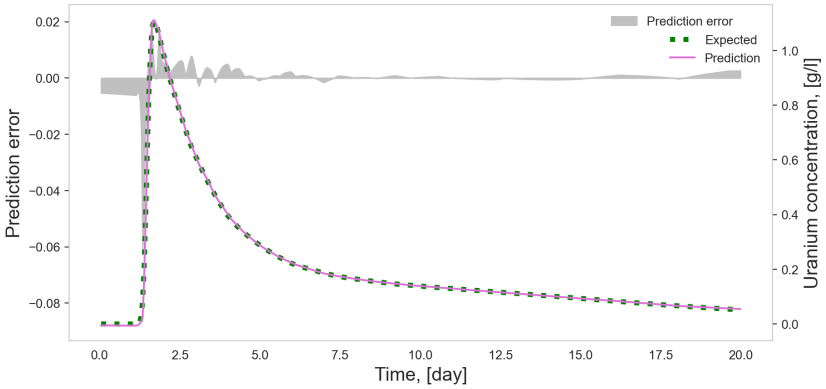


Figure 7. Extraction of uranium prediction for test case 2, with both vertical axes having different scales.

Again, the neural network predicted results similar to the results achieved with reactive transport simulation. A higher accuracy was achieved in this case, with the prediction errors in uranium concentration ranging from −0.06229 to 0.01737 mg·L^{-1}. The average error was equal to 0.00011 (0.0099%), whereas the percentage difference in total produced uranium between the expected and predicted outcomes provided by Equation (10) was 0.05429%.

Figure 8 demonstrates the predicted extraction curve of the concentration of uranium in the pregnant solution [mg·L^{-1}] per day for test case scenario 3.

Similar to the previous cases, the ANN's prediction corresponds to the prediction obtained via traditional modeling. In this case, a slight underestimation can be observed before the dissolved uranium reaches the tube, followed by an overestimation afterwards. The errors in dissolved uranium concentration ranged from −0.04493 to 0.02563 mg·L^{-1}, the average error was equal to 0.00037 (0.02596%), and the difference in the totals was 0.17981% (Table 5).

An additional test set that was not utilized during the training phase of the model was generated for evaluation and cross-validation purposes. The input parameter range was also extended beyond the scope of the training dataset, covering flow velocities from 0.45 to 0.95 m per day, reagent concentrations from 5 to 35 g per liter, and solid uranium mass concentrations ranging from 0.03% to 0.06%. In total, 216 additional test cases were

evaluated. As shown in Figure 9, the model demonstrated good robustness, with low deviations when the input parameters fall within the training dataset's range. However, significant deviations were observed for reagent concentrations at 5 g per liter, which is below the training minimum of 10 g per liter. Additionally, errors were noted for a solid uranium content below 0.00035 $kg \cdot kg^{-1}$, which was the minimum used in the training set. No consistent error patterns were identified for flow velocity values, likely due to the gradual variation of these values within the extended range.

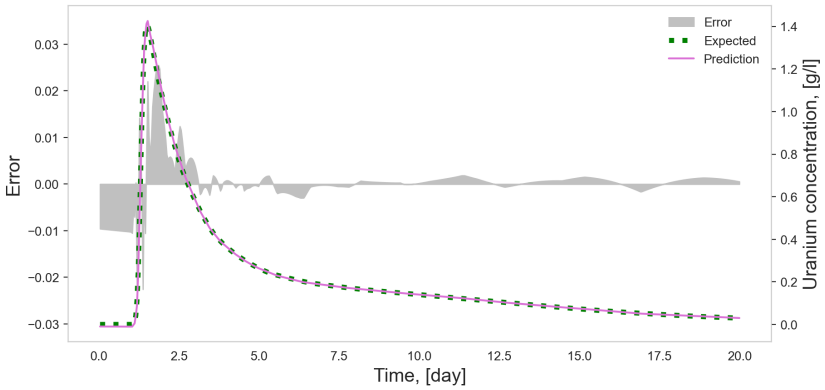


Figure 8. Extraction of uranium prediction for test case 3, with both vertical axes having different scales.

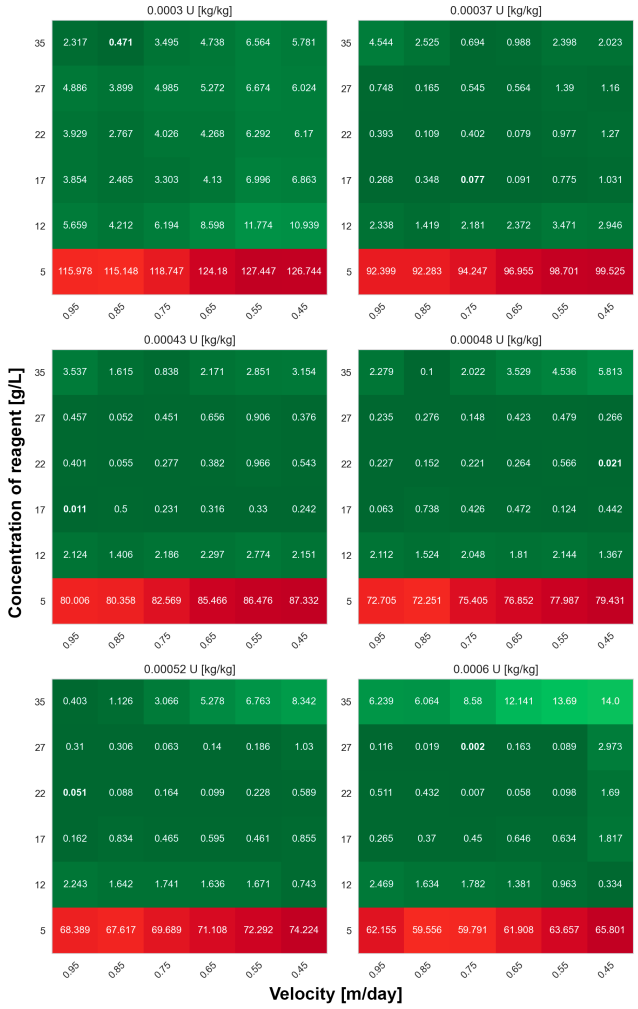


Figure 9. Percentage deviation of total uranium extraction prediction per each input parameter value within and outside the training range.

The model's performance was further investigated by changing the 'learning rate' and 'number of epochs' hyperparameters. Neural network models were trained with learning rates ranging from 0.01 and 0.1 and numbers of epochs from 10 to 1000. The resulting errors were estimated using the normalized root mean square deviation (NRMSD) function (Figure 10).

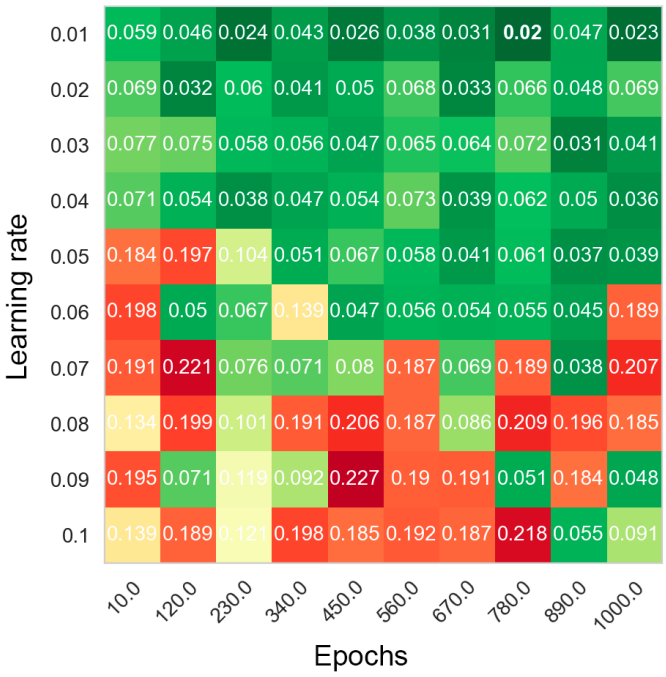


Figure 10. Normalized root mean square deviation between predicted and simulated results with different numbers of epochs and learning rate values.

As anticipated, increasing the number of epochs and reducing the learning rate resulted in improved prediction accuracy. The minimum error was achieved at a learning rate of 0.01 and 780 epochs. However, the accuracy gains became marginal beyond 900 epochs, with diminishing gains in accuracy after 900 epochs. In addition, increasing the number of epochs proportionally extends the required training time, as illustrated in Figure 11.

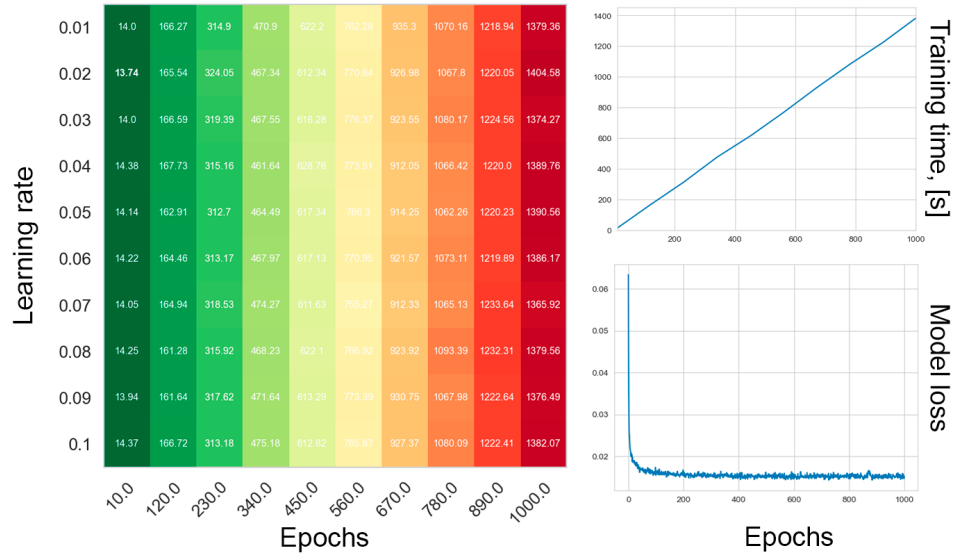


Figure 11. Training time as a function of the number of epochs and learning rate alongside the model's loss progression over 1000 epochs.

Table 5. Estimation accuracy of the ANN for the three test cases.

Test Case	ϵ_{avg}	ϵ_{avg} %	ϵ_{max}	ϵ_{max} %	Δ_{total} %
1	0.00096	0.1171	0.04493	5.48057	0.8527
2	0.00011	0.0099	0.06229	5.6054	0.85457
3	0.00037	0.02596	0.02551	1.79009	1.19986

4. Conclusions

While solutions for geomodeling, CFD, and reactive transport simulations currently exist, such as those developed by ORANO (HYTEC), Rosatom, and NAC Kazatomprom, there is a prevailing problem in the necessity for either high-performance computing clusters located off-site or extended execution times on-site. In any case, for production involving various scenarios, both of these solutions become less viable in situations requiring expedited forecasting. The current work investigates the applicability of artificial neural networks for forecasting the extraction rate of minerals produced via the In Situ Leaching (ISL) method.

This study was conducted on the basis of an experiment conducted by JSC NAC Kazatomprom involving several parameters. All intermediate steps were skipped, while an ANN was trained to provide extraction curves based on preproduction data available in databases and the eventual expected recovery degree obtained through traditional modeling techniques.

A reactive transport model was used to simulate a leaching experiment within various leaching scenarios to generate synthetic training data as a pair of datasets, namely the initial data and resulting extraction curves. The constructed ANN was trained and evaluated for the sensitivity of both accuracy and training time to the hyperparameters.

The ANN was also tested on scenarios outside of the data range used for training, with the results showing that this type of regression neural network can be applied to model the recovery rate (or extraction degree) of mineral production, specifically the ISL process. Within the designed modeling framework, the most effective combination of learning rate and number of epochs was found to be 0.01 and 780, respectively. The average absolute error for the resulting predictions was within the range of 0.00011 to 0.00096. The accuracy of the model was around 99%, although this might decrease when applied to a real technological block with an increased number of parameters.

The model evaluation was based on only five key parameters: production time, reagent concentration in the leaching solution, crystallized uranium concentration, flow velocity of the leaching solution, and expected concentration of extracted uranium. In practice, however, the ISL process is influenced by a broader range of factors, such as well locations, well screen depth, and the use of additional reagents (e.g., pyrolusite, peroxide) to accelerate leaching. Furthermore, several assumptions were made in this study; the flow velocity was considered to be constant over time, the porous medium was assumed to be homogeneous, and the reagent concentration was treated as unchanged throughout the exploitation process. These assumptions align with the controlled laboratory conditions used in the study, where the medium was crushed and the sulfuric acid concentration was maintained consistently.

The primary limitations of the model stem from its inability to account for variations in production regimes. This includes changes in the chemical composition of the leaching solution, which may fluctuate during production, as well as alterations in well flow rates and pore clogging, all of which can impact the flow velocity of the leaching solution. Additionally, the model's performance declined when the test case values fell outside of the range used during training, particularly for reagent concentration, which appears to have a pronounced effect on prediction accuracy.

Therefore, further research is required to evaluate the model using real historical data obtained from technological blocks, which incorporate a broader set of parameters. Using these data will allow us to assess the model's viability in forecasting production

for prospective technological blocks. To address the aforementioned limitations, a more sophisticated neural network architecture should be developed to accommodate changes in production regimes. This would likely involve designing the model to accept vector inputs for properties such as reagent concentrations and flow velocities, allowing it to more effectively capture temporal and spatial variations. Furthermore, the model should be able to consider the evolving geological conditions of the deposit, as pore clogging from gypsum precipitation or mechanical processes can alter flow dynamics and affect leaching efficiency.

In addition to its prevalence in uranium extraction, the ISL technique is also widely applied to recover other valuable resources, including copper, gold, and rare earth elements. By appropriately tuning a composite neural model, the current research could be adapted to quickly forecast the extraction of these components, thereby facilitating decision-making processes prior to production. This would be particularly useful for tasks such as expedited production cost estimation, optimizing operational parameters, and assessing economic feasibility.

Author Contributions: Ideas: D.A., M.T. and M.K.; methodology: D.A., M.T. and N.S.; software and tests: D.A., M.K. and N.S.; case study: M.K.; writing—original draft preparation: M.T. and D.A.; writing—review and editing: M.T. and D.A.; visualization: M.K., M.T. and N.S.; supervision: M.T.; funding acquisition: M.T. All authors have read and agreed to the published version of the manuscript.

Funding: This work was funded by the Ministry of Science and Higher Education of Kazakhstan through the Program of Targeted Financing (BR20280990).

Data Availability Statement: The original contributions presented in the study are included in the article, further inquiries can be directed to the corresponding authors.

Acknowledgments: We are grateful to the Joldasbekov Institute of Mechanics and Engineering for their support.

Conflicts of Interest: The authors declare no conflicts of interest.

References

1. Boytsov, A. Sustainable development of uranium production: Status, prospects, challenges. In Proceedings of the International Symposium on Uranium Raw Material for the Nuclear fuel Cycle: Exploration, Mining, Production, Supply and Demand, Economics and Environmental issues (URAM-2018), IAEA, Vienna, Austria, 25–29 June 2018; pp. 49–50.
2. Li, G.; Yao, J. A Review of In Situ Leaching (ISL) for Uranium Mining. *Mining* **2024**, *4*, 120–148. [CrossRef]
3. Seredkin, M.; Zabolotsky, A.; Jeffress, G. In situ recovery, an alternative to conventional methods of mining: Exploration, resource estimation, environmental issues, project evaluation and economics. *Ore Geol. Rev.* **2016**, *79*, 500–514. [CrossRef]
4. Kurmanseiit, M.B.; Tungatarova, M.S.; Kaltayev, A.; Royer, J.-J. Reactive Transport Modeling during Uranium In Situ Leaching (ISL): The Effects of Ore Composition on Mining Recovery. *Minerals* **2022**, *12*, 1340. [CrossRef]
5. Poezhaev, I.P.; Polynovsky, K.D.; Gorbatenko, O.A.; Panova, E.N.; Bulenova, K.Z.; Karmanov, E.M.; Blynsky, P.A.; Bitovt, O.A. *Geotechnology of Uranium [Geotehnologiya Urana]*; Kazakh Universitety: Almaty, Kazakhstan, 2017; 319p. (In Russian)
6. Podrezov, D.R. Development and Identification of Models for the Reserves Estimating of the URANIUM In-Situ Leaching Mine [Razrabotka i Identifikatsiya Modeley Otsenki Zapasov Rudnika Podzemnogo Skvazhinnogo Vyshchelachivaniya Urana]. Ph.D. Thesis, National Research Technological University "MISIS", Moscow, Russia, 2021. (In Russian)
7. Li, Y.; Zhang, C.; Tang, Z.; Li, C.; Liu, Z.; Tan, K.; Liu, L. Hydrodynamics control for the well field of in-situ leaching of uranium. *Nucl. Eng. Technol.* **2024**, *56*, 4176–4183. [CrossRef]
8. Li, H.; Tang, Z.; Xiang, D. Study on Numerical Simulation of Reactive-Transport of Groundwater Pollutants Caused by Acid Leaching of Uranium: A Case Study in Bayan-Uul Area, Northern China. *Water* **2024**, *16*, 500. [CrossRef]
9. Kaltayev, A.; Tungatarova, M.; Aizhulov, D.; Kurmanseiit, M.; Shayakhmetov, N.; Turar, O.; Kuchin, Y.; Yakunin, K.; Seitov, A.; Amanzholov, T.; et al. *Research Report on Intelligent Control and Decision-Making Systems for the Development of Uranium and Oil Deposits [Otchet o Nauchno-Issledovatel'skoy Rabote Intellektual'nyye Sistemy Upravleniya i Prinyatiya Resheniy Dlya Razrabotki Mestorozhdeniy Urana i Nefti]*; Al-Farabi Kazakh National University: Almaty, Kazakhstan, 2020; p. 159. (In Russian)
10. Aizhulov, D.; Shyakhmetov, N.M.; Kaltayev, A. Quantitative model of the formation mechanism of the roll-front uranium deposits. *Eurasian Chem.-Technol. J.* **2018**, *3*, 213–221. [CrossRef]
11. Abzalov, M.; Drobov, S.; Gorbatenko, O.; Vershkov, A.; Bertoli, O.; Renard, D.; Beucher, H. Resource estimation of in situ leach uranium projects. *Appl. Earth Sci.* **2014**, *123*, 70–85. [CrossRef]
12. Renard, D.; Beucher, H. 3D representations of a uranium roll-front deposit. *Appl. Earth Sci.* **2012**, *121*, 84–88. [CrossRef]

13. Aizhulov, D.; Tungatarova, M.; Kaltayev, A. Streamlines Based Stochastic Methods and Reactive Transport Simulation Applied to Resource Estimation of Roll-Front Uranium Deposits Exploited by In-Situ Leaching. *Minerals* **2022**, *12*, 1209. [CrossRef]
14. Kurmanseiit, M.B.; Tungatarova, M.S.; Royer, J.-J.; Aizhulov, D.Y.; Shayakhmetov, N.M.; Kaltayev, A. Streamline-based reactive transport modeling of uranium mining during in-situ leaching: Advantages and drawbacks. *Hydrometallurgy* **2023**, *220*, 106107. [CrossRef]
15. Tungatarova, M.S.; Kurmanseiit, M.B.; Shayakhmetov, N.M. GPU Accelerated Modeling of In-Situ Leaching Process and Streamline Based Reactive Transport Simulation. *Procedia Comput. Sci.* **2020**, *178*, 145–152. [CrossRef]
16. Panfilov, M.; Uralbekov, B.; Burkitbayev, M. Reactive transport in the underground leaching of uranium: Asymptotic analytical solution for multi-reaction model. *Hydrometallurgy* **2016**, *160*, 60–72. [CrossRef]
17. Wang, B.; Luo, Y.; Liu, J.; Li, X.; Zheng, Z.; Chen, Q.; Li, L.; Wu, H.; Fan, Q. Ion migration in in-situ leaching (ISL) of uranium: Field trial and reactive transport modelling. *J. Hydrol.* **2022**, *615*, 128634. [CrossRef]
18. Raissi, M.; Perdikaris, P.; Karniadakis, G.E. Physics-informed neural networks: A deep learning framework for solving forward and inverse problems involving nonlinear partial differential equations. *J. Comput. Phys.* **2019**, *378*, 686–707. [CrossRef]
19. Karniadakis, G.E.; Kevrekidis, I.G.; Lu, L.; Perdikaris, P.; Wang, S.; Yang, L. Physics-informed machine learning. *Nat. Rev. Phys.* **2021**, *3*, 422–440. [CrossRef]
20. Kharazmi, E.; Zhang, Z.; Karniadakis, G. hp-VPINNs: Variational physics-informed neural networks with domain decomposition. *Comput. Methods Appl. Mech. Eng.* **2021**, *374*, 113547. [CrossRef]
21. Sajjad, U.; Bibi, F.; Hussain, I.; Abbas, N.; Sultan, M.; Asfahan, H.; Aleem M.; Yan, W.; Kharazmi, E. Machine learning enabled assessment of the vacuum freeze-drying of the kiwifruit. *Inf. Process. Agric.* **2024**, *in press*. [CrossRef]
22. Wang, B.; Luo, Y.; Qian, J.; Liu, J.; Li, X.; Zhang, Y.; Chen, Q.; Li, L.; Liang, D.; Huang, J. Machine learning–based optimal design of the in-situ leaching process parameter (ISLPP) for the acid in-situ leaching of uranium. *J. Hydrol.* **2023**, *626*, 130234. [CrossRef]
23. Muhamedyev, R.I.; Kuchin, Y.I.; Muhamedyeva, E.L. Geophysical research of boreholes: Artificial neural networks data analysis. In Proceedings of the 6th International Conference on Soft Computing and Intelligent Systems, and the 13th International Symposium on Advanced Intelligence Systems, Kobe, Japan, 20–24 November 2012; pp. 825–829. [CrossRef]
24. Abassi, J.; Andersen, P. Physical activation functions (PAFs): An approach for more efficient induction of physics into physics-informed neural networks (PINNs). *Neurocomputing* **2024**, *608*, 128352. [CrossRef]
25. Cai, S.; Mao, Z.; Wang, Z.; Yin, M.; Karniadakis G.E. Physics-informed neural networks (PINNs) for fluid mechanics: A review. *Acta Mech. Sin.* **2021**, *37*, 1727–1738. [CrossRef]
26. Steefel, C.I.; DePaolo, D.J.; Lichtner, P.C. Reactive transport modeling: An essential tool and a new research approach for the Earth sciences. Earth Planet. *Earth Planet. Sci. Lett.* **2005**, *240*, 539–558. [CrossRef]
27. Bear, J. *Dynamics of Fluids in Porous Media*; Dover Publications Inc.: New York, NY, USA, 2014; 757p.

Disclaimer/Publisher's Note: The statements, opinions and data contained in all publications are solely those of the individual author(s) and contributor(s) and not of MDPI and/or the editor(s). MDPI and/or the editor(s) disclaim responsibility for any injury to people or property resulting from any ideas, methods, instructions or products referred to in the content.